25th ABCM International Congress of Mechanical Engineering
October 20-25, 2019, Uberlândia, MG, Brazil

COB-2019-1465
ANALYTICAL AND NUMERICAL STUDY OF RADIATION IN HEAT SINKS OF RECTANGULAR FINS

Felipe Henrique Rafael
Vilson Altair da Silva
Bruno de Campos Salles Anselmo
Sandro Metrevelle Marcondes de Lima e Silva
Universidade Federal de Itajubá – Campus Prof. José Rodrigues Seabra, Av. BPS, 1303, Bairro Pinheirinho, Itajubá – MG.
fhrafael095@gmail.com, altairvilson@gmail.com, brunocsa@gmail.com, metrevel@unifei.edu.br

Abstract. *The objective of this study is to present an analytical model for the determination of the thermal radiation in heat sinks of rectangular base and fins, and to verify the influence of geometric parameters and the emissivity on the net radiation heat flux. The analytical model used establishes a view factor that assumes a uniform radiosity surface. The influence of this hypothesis was analyzed through a numerical study using the software COMSOL Multiphysics®. The radiation study was performed in 6 heat sinks varying in height and spacing of the fins, which radiosity changes along the surface were considered. The results for the analytical and numerical model presented good accordance, providing a maximum relative deviation of 5.5%. On the other hand, the omission of the view factor was also evaluated, resulting in a maximum deviation of 104.8% in relation to the numerical data. Finally, a diagram was proposed relating the geometric parameters, the emissivity and the view factor. With this diagram is possible to extend the analysis, providing a general interpretation of the radiation in function of the dimensions and the emissivity, an alternative approach for the determination of the view factor of the heat sinks of rectangular fins.*

Keywords: *heat sinks, thermal radiation, view factor, COMSOL.*

1. INTRODUCTION

Heat sinks are widely used in engineering systems that require cooling as they are presented as a cost-effective and robust way of promoting heat removal, clear from mobile parts and noise. These devices aim to increase the heat transfer with the surroundings in order to guarantee the operation temperature of the systems in which they are applied. Several studies have been investigating the heat transfer between heat sinks and the external environment. However, the authors have often neglected the effect of radiation in their studies, such as: Harahap and Lesmana (2006), Yazicioğlu and Yüncü (2009) and Meng et al. (2018) or did not consider the effect of the view factor on the radiation analysis as in Sasikumar et al. (2002) and Rao et al. (2007).

Yu et al. (2010) studied radial heat sinks using pure polished Al with emissivity equal to 0.1 and they neglected the radiation effect, since the radiant flux was less than 5% of the total heat flux due to the low emissivity. On the other hand, Abramzon (1997) and, more recently, Rao et al. (2006) stated that the thermal radiation from hot surfaces to the environment can account for up to 20% of the total heat dissipated by the heat sink. In another study using radial heat sinks, Yu et al. (2011) observed a maximum contribution of 27% in the total heat transfer. Thus, the omission of radiation effects does not apply to most heat sinks that seek to increase the exchange by radiation, which would make the data inaccurate.

Kobus and Oshio (2005) reported that one of the main reasons for excluding the effects of thermal radiation on the analysis of finned surfaces may be attributed to the difficulty in determining the view factor. However, some studies have demonstrated methodologies that consider the geometry in the determination of radiation. Ellison (1979) modeled an equivalent circuit and considered the gray body model to determine the view factor from a rectangular U-channel. Some curves were plotted to help the heat sink designer evaluate the heat transfer rate by radiation to a variety of dimensions and emissivities. The results already showed the existence of gross errors in some data published previously and in common methods in the electronic industry until then.

More recently, Shabany (2008) proposed an approximate correlation to determine the radiation, from the exact solution on rectangular fin heat sinks, and compared the results for various dimensional relationships, which resulted in a maximum error of 11%.

Khor et al. (2010) experimentally investigated the importance of the thermal radiation effects and theirs corresponding view factor on the thermal performance of a rectangular fin heat sink horizontally positioned under natural convection.

They observed that the procedure of neglecting the view factor in the analysis of thermal radiation in heat sinks should not be used because the errors generated are noticeably greater than those of just neglecting thermal radiation.

Yu et al. (2011) studied radial heat sinks, considering both natural convection and radiation. The authors verified that the radiation had a significant effect on the optimal fin length as a function of the heat sink performance. They emphasized that the heat transfer by radiation depends on the emissivity, the view factor and the temperature, while the emissivity depends on the surface treatment, the view factor is determined by the geometry, and the surface temperature depends on the room temperature and the heat flux. They concluded, therefore, that emissivity, view factor and temperature should be considered to accurately analyze the radiation heat transfer.

The present study intends to investigate, in a general way, the influence of the omission of the view factor in the determination of the thermal radiation in heat sinks of rectangular base and fins. Besides, a diagram is proposed to obtain the view factor elaborated from analytical equations. The development of the analytical solution is done by considering the heat sink a gray surface model, diffuse, opaque, isothermal and with uniform radiosity. Where it is verified that only the latter is not a reasonable approximation for the applications in general. Thus, the deviation caused by the use of the uniform radiosity hypothesis was investigated based on 6 heat sinks from Silva (2015), which differ in height dimensions and fin spacing. The results of the analytical model applied to the heat sinks analyzed, as well as, a model that omits the view factor, were compared with the data provided by COMSOL. The validity of the analytical model and the implications of the omission of the view factor are discussed based on the relevant parameters that determine them.

2. THERMAL RADIANTION THEORY

2.1 Radiation on real surfaces

Incropera et al. (2008) define thermal radiation as the energy emitted from materials that is at a non-zero temperature, which can be attributed to changes in the electronic configurations of the atoms or molecules that constitute it. The transport of this form of energy is done by electromagnetic waves, or alternatively photons, so that, unlike conduction and convection heat transfer requiring a material medium, radiation does not need it.

The radiation emitted by a surface has its origin in the thermal energy of the material delimited by the surface, and the rate at which the energy is released per unit area is known as emissive power, E, of the surface. The Stefan-Boltzmann's Law determines an upper limit for that emissive power defined by Eq. (1), which corresponds to the emission of a blackbody, E_n, where T is the absolute surface temperature and σ is the constant of Stefan-Boltzmann $\sigma = 5.67 \times 10^{-08}$ W/m^{2}K.

$$E_n = \sigma T^4 \tag{1}$$

The thermal flux emitted by an actual surface is smaller than that emitted by a blackbody at the same temperature and is given by Eq. (2), where ε is a surface property known as emissivity, with values varying in the range of $0 \leq \varepsilon \leq 1$.

$$E = \varepsilon \sigma T^4 \tag{2}$$

Radiation can also reach a surface from its surroundings. The rate at which all radiation coming from the external environment and incident on the surface is called irradiation, G. A portion, or all irradiation, can be absorbed by the surface, thereby increasing the thermal energy of the material. The rate at which radiation is absorbed per unit area can be calculated with the knowledge of a surface property called absorbance, α, whose values are also present in the range $0 \leq \varepsilon \leq 1$. When the surface is opaque, the portion of the irradiation that has not been absorbed is reflected. Therefore, we can define a third property called reflectivity, ρ, where the relation established in Eq. (3) becomes valid.

$$\alpha + \rho = 1 \tag{3}$$

In this way, emissivity is defined as the ratio of the radiation emitted by the surface to the radiation emitted by a blackbody at the same temperature. Absorptivity, in turn, is the fraction of the radiation that is absorbed by a surface. However, the shape of the spectral distribution radiation differs from the shape of the distribution of a blackbody, and the emissivity varies depending on the region of the spectrum. On the other hand, a surface may absorb the incident radiation preferably at certain wavelengths. In addition, the directional distribution may not be diffuse, meaning that its value will undergo variations with direction.

In general, spectral directional emissivity $\varepsilon_{\lambda,\theta}$ is the ratio of the radiation emitted at a temperature, wavelength and direction, and the radiation emitted by a blackbody at the same temperature and wavelength. Similarly, the spectral directional absorptivity $\alpha_{\lambda,\theta}$ is described as the fraction of the radiation at a given wavelength, incident in a certain direction, which is absorbed by the surface. Such properties can conveniently be presented by their means in all directions and possible wavelengths, which respectively defines the total hemispherical emissivity, ε, and the total hemispherical absorptivity, α.

An important relation of equivalence between the absorptivity and emissivity derives from the Kirchhoff's Law, which is based on an energy balance applied to a surface under diffuse irradiation and equivalent to the blackbody emission in

steady regime, which should result in the equivalence between absorption and emission rates. One result of this law is that the total hemispherical emissivity of a surface under such conditions corresponds numerically to its total hemispherical absorptivity. Despite the diffuse irradiation restriction for the application of this equivalence, a similar logic can be used which results in a form of the unrestricted Kirchhoff's Law, characterized by the equivalence between the directional spectral properties, as expressed in Eq. (4).

$$\varepsilon_{\lambda,\theta} = \alpha_{\lambda,\theta} \tag{4}$$

This equality is always applicable because they are inherent properties of the surface. In the case of a diffuse surface, the emissivity and the absorptivity are independent of the direction. In addition, if it is possible to assume the gray sufarce model, whose properties referred to are independent of the wavelength, it follows that $\varepsilon_{\lambda,\theta} = \varepsilon$, and $\alpha_{\lambda,\theta} = \alpha$. This result implies in the condition expressed $\varepsilon = \alpha$.

Normal surface emissivity values ε_n are widely available in the literature and in catalogs for common surface finishing conditions in various materials. If the surface does not exhibit a diffuse behavior, the total hemispherical emissivity ε will diverge from that provided to normal direction. However, according to Incropera et al. (2008), this variation will often be small, and the diffuse surface model will generally be a reasonable approximation, because, according to the authors, although there are preferential directions for emission, hemispherical emissivity ε will not differ markedly of the normal emissivity ε_n, rarely being outside the range $1.0 \leq \varepsilon/\varepsilon_n \leq 1.3$ in conductive materials.

As for the gray surface model, it is not necessary that α and ε be independent of λ over the entire spectrum, but only in the emission and irradiation spectral regions of surface. Attention should be drawn to the characterization of this model, especially when the spectral regions of emission and irradiation are very far apart, since the absorption would occur in one region of the spectrum and the emission in another region, which could imply the divergence between emissivity and absorptivity.

However, due to the high conductivity of the heat sinks material, the surface temperature is almost uniform. Additionally, it has been found that the irradiation on the surface of the heat sink comes in part from itself. Thus, the spectral regions for emission and irradiation will be practically coincident. The other part of the irradiation originates in the vicinity, and corresponds to the emission of a black body, since its dimensions are much larger than those of the heat sink, which characterizes the hypothesis for the application of Kirchhoff's Law that results in the same relation than the gray surface model. Consequently, the gray surface model becomes reasonable for heat sink applications, since the actual condition approaches the hypotheses used in its characterization.

2.2 Radiation exchange on finned surfaces

The surface radiosity, by definition, represents the total rate of radiation leaving a surface, constituting a portion of emission and another of reflection by incident radiation (irradiation), G_i, according to Eq. (5). The view factor $F_{i,j}$ is defined as the radiation fraction leaving the surface i and intercepted by the surface j. Assuming that i emits and reflects diffusely and considering that the radiosity J_i is uniform along surface i, so $F_{i,j}$ can be expressed by Eq. (6), where R is the distance between the elementary surfaces dA_i and dA_j; θ_i and θ_j are the respective angles formed between their normal and the line segment that joins them.

$$J_i = E_i + \rho_i G_i \tag{5}$$

$$F_{ij} = \frac{1}{A_i}\int_{A_i}\int_{A_j}\frac{\cos\theta_i \cos\theta_j}{\pi R^2} dA_i dA_j \tag{6}$$

Through a balance of thermal exchange by radiation on surface i, one can write generally the expression determined by Eq. (7), in which the net amount of energy leaving a surface, Q_i, corresponds to the difference between all energy which leaves the surface i, defined by its radiosity J_i, and the energy incident on the surface, defined by its irradiation G_i.

$$Q_i = A_i(J_i - G_i) \tag{7}$$

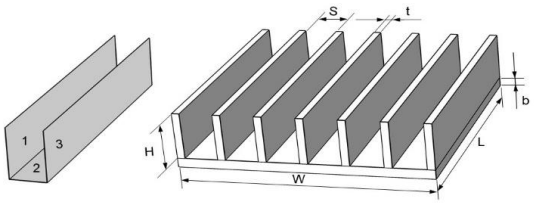

a) b)

Figure 1. (a) Schematic channel of heat sink (b) Heat sink parameters of dimensions.

A heat sink is composed of fins commonly arranged according to Fig. 1(b). Each pair of adjacent fins forms a channel whose surfaces partially block the flow of radiation therein, such that part of the emitted energy is reabsorbed, and only

a portion is lost to the vicinity. The other surfaces of the heat sink, external to the channels, interact only with the environment, so all the radiation emitted in these regions will be lost to the surroundings.

3. RADIATION MODELS

3.1 Development of the analytical equations

If the gray, diffuse and opaque surface model is applicable, the relations determined by Eqs. (1-3), and $\varepsilon = \alpha$ are employed, so that Eq. (5) can be rewritten according to Eq. (8), where T_i is the temperature, ε_i is the emissivity of the surface.

$$J_i = \varepsilon_i \sigma {T_i}^4 + (1 - \varepsilon_i) G_i \tag{8}$$

Replacing the resulting expression J_i in Eq. (7) yields an expression relating the emission of a surface, its radiosity, and the emission of a blackbody at the same temperature through Eq. (9). By making a balance of radiation energy flux between surfaces composing a cavity, it can be established that the energy portion $Q_{i,j}$ emitted by a surface i that is intercepted by another surface j, is determined by Eq. (10), where A_i corresponds to the area of the emitter surface i, J_i and J_j represent the radiosity of the surfaces i and j respectively, and $F_{i,j}$ represents the view factor between the surfaces, defined for isothermal surfaces and uniform radiosity surfaces.

$$Q_i = \frac{A_i \varepsilon_i (\sigma {T_i}^4 - J_i)}{1 - \varepsilon_i} \tag{9}$$

$$Q_{ij} = A_i F_{ij} (J_i - J_j) \tag{10}$$

The sum of the radiation portions from a surface i due to its emission and incident on each surface j that composes the cavity is equal to the total emitted by the surface i. This allows to define the expression given by Eq. (11), thus relating Eq. (9) and Eq. (10), where n_s is the number of cavity surfaces.

$$Q_i = \sum_{j=1}^{n_s} Q_{ij} \;\Rightarrow\; \frac{\sigma {T_i}^4 - J_i}{(1 - \epsilon_i)/A_i \epsilon_i} = \sum_{j=1}^{n_s} \frac{J_i - J_j}{(A_i F_{ij})^{-1}} \tag{11}$$

Considering, in principle, the energy exchanged between each channel and the environment, it assumes a model consisting of a cavity of two surfaces, where one surface corresponds to the channel and the other to the surroundings. Thus, we can determine the total radiosity of the channel by applying Eq. (11) to the two surfaces, resulting in the system of linear equations expressed by Eq. (12).

$$\begin{bmatrix} F_{12} + \varepsilon_1/(1 - \varepsilon_1) & -F_{12} \\ -F_{21} & F_{21} + \varepsilon_2/(1 - \varepsilon_2) \end{bmatrix} \cdot \begin{bmatrix} J_1 \\ J_2 \end{bmatrix} = \sigma \begin{bmatrix} [\varepsilon_1/(1 - \varepsilon_1)] {T_1}^4 \\ [\varepsilon_2/(1 - \varepsilon_2)] {T_2}^4 \end{bmatrix} \tag{12}$$

The resulting expressions to J_1 and J_2, when being substituted in Eq. (9), and assigned reciprocal relations between the view factors F_{12} F_{12} and F_{21}, provide Eq. (13).

$$Q_1 = -Q_2 = \frac{\sigma({T_1}^4 - {T_2}^4)}{(1 - \varepsilon_1)/A_1 \varepsilon_1 + 1/A_1 F_{12} + (1 - \varepsilon_2)/A_2 \varepsilon_2} \tag{13}$$

Thus, by defining the surface characterized by the index 1 as the surface of the channel, and consequently the surface 2 as the surrounds, the expression can be simplified, since the area of the vicinity surface in general is much larger than the other dimensions involved, which makes the third installment of the denominator negligible. Changing the indexes $Q_1 = Q_c$, $A_1 = A_c$, $\varepsilon_1 = \varepsilon$, $T_1 = T$ e $T_2 = T_\infty$, the expression results in Eq. (14).

$$Q_c = \hat{F} A_c \sigma (T^4 - {T_\infty}^4) \tag{14}$$

where $\hat{F}$ is defined, according to Ellison (1979), as:

$$\hat{F} = \frac{1}{(1 - \varepsilon)/\varepsilon + 1/F_C} \tag{15}$$

The calculation of the channel view factor for surround, F_c, can be done by subdividing the surface of the channel in flat surfaces according to Fig. 1(a), and applying reciprocity and sum relations to the view factor according to the development in Eq. (16).

$$
\begin{aligned}
&F_C = 1 - F_{123-123} \\
&= 1 - (F_{123-1} + F_{123-2} + F_{123-3}) \\
&= 1 - (2F_{123-1} + F_{123-2}) \\
&= 1 - [(2A_1/A_{123})F_{1-123} + (A_2/A_{123})F_{2-123}] \\
&= 1 - [(2\,A_1/A_{123})(F_{1-1} + F_{1-2} + F_{1-3}) + (A_2/A_{123})(F_{2-1} + F_{2-2} + F_{2-3})] \\
&= 1 - [(2\,A_1/A_{123})(F_{1-2} + F_{1-3}) + (A_2/A_{123})(2F_{2-1})] \\
&= 1 - A_1/A_{123}\,(4F_{1-2} + 2F_{1-3}) = 1 - \tfrac{H}{2H+S}(4F_{1-2} + 2F_{1-3})
\end{aligned}
\tag{16}
$$

Incropera et al. (2008) presents the solution of Eq. (6) for parallel and perpendicular flat surfaces. In this way, we can determine F_{1-2} and F_{1-3} respectively by means of Eq. (17) and Eq. (18), where $\bar{S} = {}^{S}/_{L}$, $\bar{H} = {}^{H}/_{L}$, $\bar{L} = {}^{L}/_{S}$ e $\bar{W} = {}^{H}/_{S}$ based on the dimensions defined in Fig. 1(b).

$$
F_{1-2} = \frac{1}{\pi\bar{S}}\left\{\bar{S}\tan^{-1}\frac{1}{\bar{S}} + \bar{H}\tan^{-1}\frac{1}{\bar{H}} - (\bar{H}^2 + \quad \bar{S}^2)^{\frac{1}{2}}\tan^{-1}\frac{1}{(\bar{H}^2+\bar{S}^2)^{\frac{1}{2}}}\right.
$$

$$
\left. + \frac{1}{4}\ln\left[\left(\frac{(1+\bar{S}^2)(1+\bar{H}^2)}{(1+\bar{S}^2+\bar{H}^2)}\right)\left(\frac{\bar{S}^2(1+\bar{S}^2+\bar{H}^2)}{(\bar{S}^2+\bar{H}^2)(\bar{S}^2+1)}\right)^{\bar{S}^2}\left(\frac{\bar{H}^2(1+\bar{S}^2+\bar{H}^2)}{(\bar{S}^2+\bar{H}^2)(\bar{H}^2+1)}\right)^{\bar{H}^2}\right]\right\} \tag{17}
$$

$$
F_{1-3} = \frac{2}{\pi\bar{L}\bar{W}}\left\{\ln\left[\frac{(1+\bar{L}^2)(1+\bar{W}^2)}{1+\bar{W}^2+\bar{L}^2}\right]^{\frac{1}{2}} + \bar{L}(1+\bar{W}^2)^{\frac{1}{2}}\tan^{-1}\frac{\bar{L}}{(1+\bar{W}^2)^{\frac{1}{2}}} + \bar{W}(1+\bar{L}^2)^{1/2}\tan^{-1}\frac{\bar{W}}{(1+\bar{L}^2)^{1/2}} - \bar{L}\tan^{-1}\bar{L} - \bar{W}\tan^{-1}\bar{W}\right\} \tag{18}
$$

The total radiation emitted by the heat sink corresponds to the sum of the radiation emitted by the channels with the radiation emitted by the heat sink regions external of channels, according to Eq. (19), where Q_t is the total net flux of energy leaving the heat sink surface by radiation; Q_c is the total net flux of energy emitted by all channels; A_{ext} is the area of the heat sink surfaces that do not make up the channels; e, A_c corresponds to the summed areas of the channels.

$$
Q_t = Q_c + \varepsilon A_{ext}\sigma\left(T^4 - T_\infty{}^4\right) = \left(\hat{F}A_c + \varepsilon A_{ext}\right)\sigma\left(T^4 - T_\infty{}^4\right) \tag{19}
$$

By defining an emission factor F as the fraction of the radiation emitted by the heat sink surface that reaches the vicinity, we obtain Eq. (20), where A_t is the total area of the heat sink, equivalent to the sum of A_c and A_{ext}.

$$
Q_t = FA_t\varepsilon\sigma\left(T^4 - T_\infty{}^4\right) \tag{20}
$$

Combining Eq. (19) and Eq. (20), and regrouping some terms, F may be obtained explicitly as:

$$
F = (A_c/A_t)\left(\hat{F}/\varepsilon - 1\right) + 1 \tag{21}
$$

3.2 Numerical study on surfaces of non-uniform radiosity

In the development of the equations, an approximation for uniform radiosity was considered in the definition of the view factor established in Eq. (6). However, in order to verify the analytical model, the numerical study was carried out using the COMSOL Multiphysics® software, taking into account the variations of radiosity along the surface on the heat sink.

The study was carried out using 6 heat sinks with base dimensions of 100 mm x 100 mm (Silva, 2015), where 3 different heights for 2 different spacing values were used. The heat sinks as well as their dimensions are shown in Tab. 1 according to the dimensions shown in Fig. 1(b).

Table 1. Heat sinks dimensions.

Heat sink	L [mm]	S [mm]	H [mm]	t [mm]	n	At [m²]
D1	100	14.35	7	2	7	0.020006
D2	100	14.35	14	2	7	0.030002
D3	100	14.35	20	2	7	0.038570
D4	100	5.55	7	2	14	0.030007
D5	100	5.55	14	2	14	0.049999
D6	100	5.55	20	2	14	0.067135

The basic division of the simulation process consisted of the preprocessing stage, which includes modeling the problem, inserting the geometric data of the structure, the constants of material, the types of elements and the mesh to be used; processing stage where the numerical operations were performed from the input data established in the pre-

processing phase; and the post-processing where the results were extracted. From a practical way, the modeling workflow followed the steps:

1. The geometry was defined, generating a model with the dimensions proposed (Tab. 1).
2. Assignment of the material to be used, adopting Al 6063-T5 as available in Silva (2015), whose reported emissivity corresponds to 0.23.
3. The *Heat Transfer module* was selected with the *surface-to-surface radiation* option.
4. The boundary condition *Diffuse surface* was defined, which assigns the gray and diffuse surface model. In addition, the temperature condition prescribed on the surface was used, since the temperatures along the heat sink, in general, did not present great variations due to the high thermal diffusivity of the material, according to the results presented by Silva (2015).
5. A tetrahedral mesh is assigned to the model. A mesh refinement study by means of convergence analysis of the results was done in each case, in order to guarantee the invariability of the numerical results in relation to the mesh.

The region where the boundary conditions of diffuse surface and prescribed temperature were imposed, as well as the mesh used in the model solution are shown in Figs. 2(a) and 2(b), respectively. The arrows in Fig. 2(a) indicate the direction of emission normal to the surface.

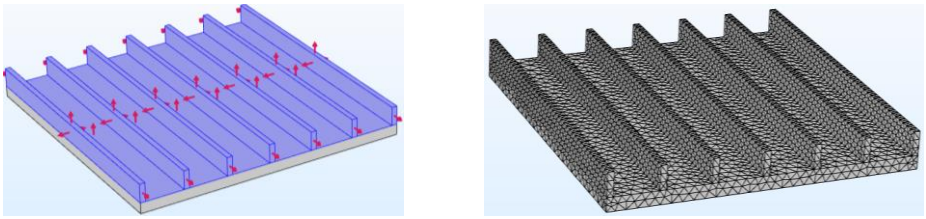

(a) (b)

Figure 2. (a) Diffuse surface boundary condition (b) Tetrahedra mesh applied on model.

The ambient temperature was set at 22ºC, following the average ambient temperatures established by Silva (2015). The applied method is called *hemicube*, which works similarly to the rendering of digital images in five different directions (in 3D, in 2D only three directions are necessary) and counts the pixels in each element of mesh to evaluate its view factor.

Its accuracy can be influenced by the resolution setting, where the number of pixels set is equal to the resolution specified squared. Thus, the time required to evaluate the radiation increases quadratically with the resolution. The default value of 256 was retained since the returned results were the same when considering higher resolutions.

4. RESULTS AND DISCUSSION

Figures 3(a) and 3(b) illustrate the radiosity distribution in the heat sinks D1 and D6, respectively, resulting from the simulation. This behavior is due to variations in the irradiation, which influences the portion of energy reflected, since in this case the emission is uniform due to the surface being isothermal.

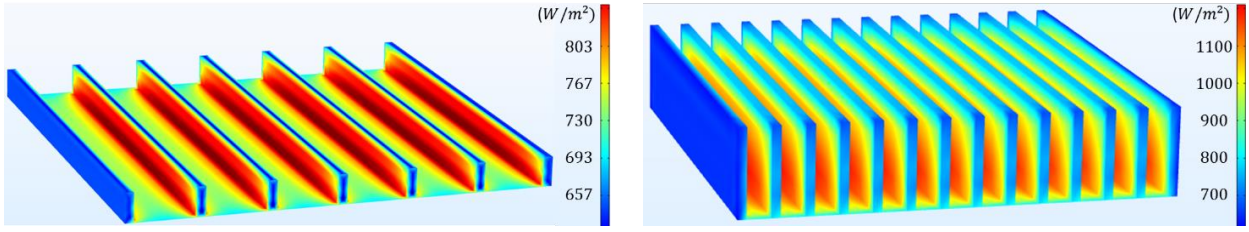

(a) (b)

Figure 3. Surface radiosity distribution for the (a) Heat sink D1 and the (b) Heat sink D6.

As established by Eq. (21), the emission factor F was determined for each heat sink presented in Tab. 1, considering A_t as the total area normally subjected to convection, equivalent to the region highlighted in Fig. 2(a) of the numerical model. These values were used to determine the radiation heat lost to the ambient by means of Eq. (20). The influence of the uniform radiosity hypothesis assumed on the analytical development was verified when comparing with the results of radiation obtained numerically. For this, the percentage deviations of the data obtained analytically with respect to the values provided by COMSOL were calculated, and the deviation was also determined for the case where F was omitted from Eq. (20), which corresponds to neglecting the view factor effects, and assume F_c, determined in Eq. (16), as being 1. Table 2 lists the deviations obtained for each heat sink analyzed as well as provides the respective calculated view factor values. The results for the net radiation heat flux are shown graphically in Figs. 4(a) and 4(b), respectively for the D1 and D6 heat sinks, as a function of the temperature difference θ between the surface of the heat sink and the

environment. These heat sinks presented, respectively, the largest and the smallest view factor among the heat sinks analyzed.

Table 2. Results of the emission factor F and relative deviation of the radiation.

Heat sink	F	With View Factor	No View Factor
D1	0.8563	0.4%	17.2%
D2	0.7728	0.6%	30.2%
D3	0.7259	1.4%	39.7%
D4	0.7094	0.1%	40.8%
D5	0.5785	3.0%	78.0%
D6	0.5151	5.5%	104.8%

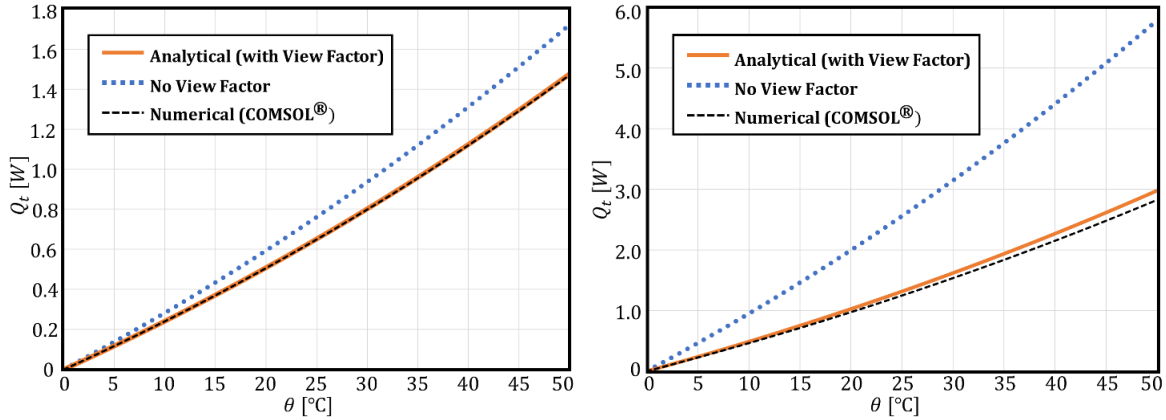

Figure 4. Comparison between the heat rate by radiation for the different models (a) Heat sink D1 and (b) Heat sink D6.

Based on the behavior of the radiation emission curves in Fig. 4, there is a good correspondence between the numerical and analytical data. On the other hand, omission of the view factor provided grossly divergent radiation data. It is concluded, therefore, that the view factor omission could produce inconsistent results, and that its use is satisfactory even if it is based on a surface model with uniform radiosity that is not verified in practice, because the errors produced will be small as verified in the results provided by COMSOL.

In order to generalize the analysis, were raised the curves presented in Fig. 5, which provide the factor *F*, defined by Eq. (21) for heat sinks of rectangular base and rectangular fins, directly by the input of dimensionless geometric parameters defined by the *H/S*, *L/S* and A_c/A_t, and by the emissivity ε. The diagram depicts the general behavior of the view factor of channels F_c and the general factor *F*, as well as providing an alternative means for obtaining them.

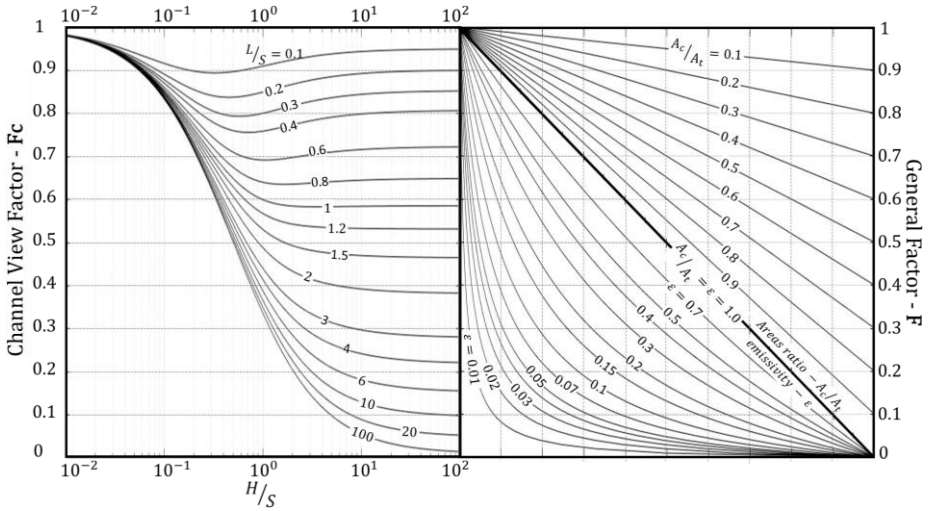

Figure 5. Generalized diagram for the view factor.

Table 3 provides the values of these dimensionless parameters for the heat sinks analyzed and presents the value of *F* calculated directly by Eq. (21), as previously presented in Tab. 2. Through the dimensionless parameters, the determination of the factor *F* can be made directly through the diagram, as shown in Fig. 6. The left quadrant will provide

a point determined by the *H/S* coordinate and the *L/S* curve whose ordinate represents the parameter A_c calculated by Eq. (16). The projection of the point is followed by a horizontal line which will determine a second point at the intersection with the emissivity curve of the material. A new projection through a vertical line will result in a third point at the intersection with the curve determined by the ratio between the summed area of the channels, A_c, and the total area of the heat sink, A_t, at which the value of the factor *F* can be read directly in the vertical axis to the right of the diagram. The verification of the values of *F* obtained in the diagram is made from the calculated values.

Table 3. Dimensionless parameters for diagram input.

Heat sink	H/S	L/S	ε	Ac/At	F (calculated)
D1	0.49	6.97	0.23	0.85	0.8563
D2	0.98	6.97	0.23	0.85	0.7728
D3	1.39	6.97	0.23	0.85	0.7259
D4	1.26	18.02	0.23	0.85	0.7094
D5	2.52	18.02	0.23	0.87	0.5785
D6	3.60	18.02	0.23	0.88	0.5151

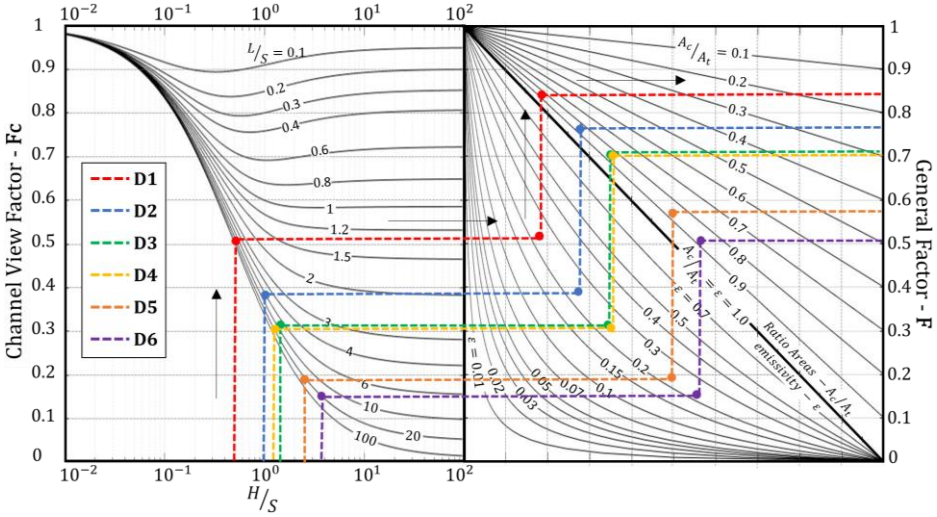

Figure 6. Scheme to obtain the factor *F* to the heat sinks analyzed.

The general view provided by the diagram of Fig. 5 also allows a qualitative evaluation of the relationships that determine the emission factor *F*. The area outside the channels contributes to its increase, since there is no obstruction to the radiation leaving its surface. Thus, smaller ratios between the total channel area and the total heat sink area will to imply an increase in view factor. However, it was observed that the variation of this parameter was minimal for the considered heat sinks, so that the most significant contribution resulted from the channel dimensions since the emissivity considered was the same in all cases. However, it is noted that the increase in emissivity induces a decrease in *F*, while smaller emissivity, less than 0.05, generally provides values close to 1. This fact justifies the omission of the view factor in some studies that have made use of highly polished surfaces such as found in Yu et al. (2010), which have low emissivity, besides the fact of this implies low radiation heat rates.

As already seen in the heat sinks analyzed, there is a reduction of the channel view factor which tends to stabilize as the height of the fins, *H*, is increased or the spacing, *S*, is reduced. On the other hand, to some extent, the ratio between the length *L* and the spacing will have a significant effect on heat sinks of small length with respect to spacing such that when *L/S* > 100, there will be practically no variation. This verification is most evident in Fig. 7, where the geometric aspect of the channels is shown in each region of the diagram. The shaded region encompasses most of the dimensions used in practice, as well as, the heat sinks presented in literature, which have been exhaustively analyzed in several dimensional configurations, such as: in Harahap and Rudianto (2005), Harahap and Lesmana (2006), Dialameh et al. (2008), Yazicioğlu and Yüncü (2007), Mehrtash et al. (2013), Shen et al. (2014) and Meng et al. (2018).

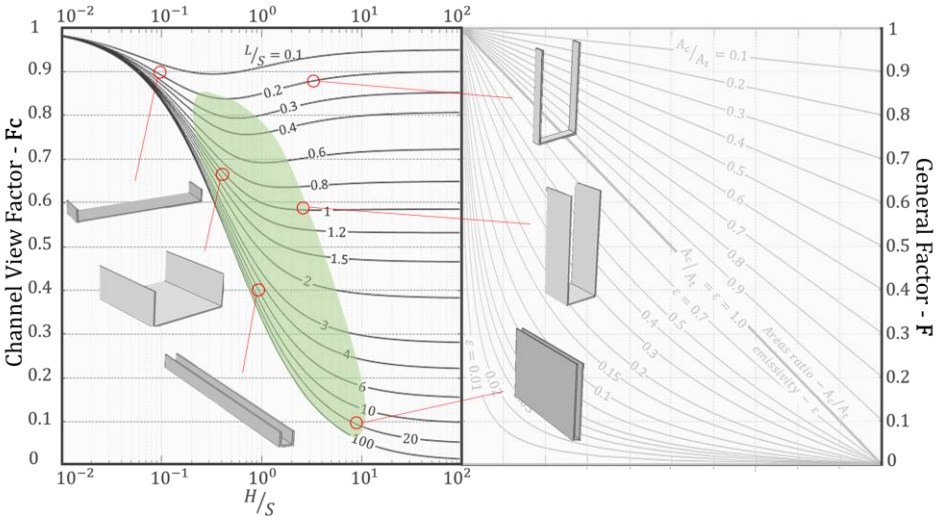

Figure 7. Geometric aspect of channels for each region

5. CONCLUSIONS

The influence of the view factor omission in determining the net radiation heat flux in heat sinks of rectangular base and fins was analyzed. An analytical model was established for gray, diffuse, opaque surfaces, isothermal surface and with uniform radiosity. Among the conditions imposed on the model, it was found that the first four were reasonable approximations, while the latter did not apply, since the radiosity had great influence on the origin irradiation in the heat sink itself, implying in a non-uniform distribution of radiosity over the surface.

The validation of the model on real surfaces of variable radiosity was done through a study where the analytical equations were applied in 6 heat sinks, varying spacing and height of the fins. In order to do so, numerical models were used through COMSOL software, where variations of radiosity in the surface of the heat sinks were considered, thus providing parameters for the comparison of the analytical model.

Through the radiation emitted curves as a function of the temperature difference θ between the heat sink surface and the environment, there was a good accordance between the results generated by the two models, so that the maximum deviation concerning the model in COMSOL was 5.5% for D6 heat sink, and a minimum of 0.1% for D4 heat sink. In parallel, the radiation was calculated analytically, however, omitting the view factor. In this case the deviations reached a maximum value of 104.8% for D6 heat sink and a minimum of 17.1% for the heat sink D1. These results indicate that the view factor omission can be problematic because, in doing so, the calculated radiation emission rate reached values above double the value provided by COMSOL to D6 heat sink, so that, the error committed for this heat sink would be less if the radiation were totally neglected.

Finally, the analysis could be generalized to diverse geometries by means of the elaboration of a diagram that provides the emission factor F that includes the view factor effects from dimensionless parameters, obtained through the heat sink dimensions and the emissivity of the material which constitutes it. It became evident that the geometric dimensions of the channel strongly influence the net radiation heat rate leaving the heat sink. In general, heat sinks with smaller heights, larger spacings and smaller lengths have larger view factors, which implies that their omission will not lead to large deviations. Otherwise, the analysis should include the view factor, and the diagram can be used as a tool to obtain it.

It was also verified that the channel view factor, F_c, tends to stabilize from certain values assigned to the dimensionless parameters. The variations in the L/S ratio to values above 50 practically do not imply any change to the view factor. In contrast, the view factor receives little influence of the H/S values when located above 10. It is also observed that the increase of the emissivity in general produces a reduction of the view factor, whereas small emissivity, smaller than 0.05, provide values of F close to 1 for the frequently used geometric relations, as indicated by Fig. 7. However, typical values of emissivity are above 0.1, implying the need to verify the view factor to obtain consistent data.

6. ACKNOWLEDGEMENTS

The authors would like to thank CNPq, FAPEMIG and CAPES for their financial support.

7. REFERENCES

Abramzon, B.M., 1997. “A simple closed-form solution for evaluation of radiative heat transfer from a rectangular fin array”. *IEEE Transactions on Components, Packaging, and Manufacturing Technology: Part A*, Vol. 20(2), pp. 225-229.

Dialameh, L., Yaghoubi, M., Abouali, O., 2008. “Natural convection from an array of horizontal rectangular thick fins with short length”. *Applied Thermal Engineering*, Vol. 28, pp. 2371–2379.

Ellison, G.N., 1979. "Generalized computations of the gray body shape factor for thermal radiation from a rectangular U-channel". *IEEE Transactions on Components, Hybrids, and Manufacturing Technology*, Vol. 2(4), pp. 517–522.

Harahap F., Lesmana, H., Dirgayasa, I.K.T.A.S., 2006. "Measurements of heat dissipation from miniaturized vertical rectangular fin arrays under dominant natural convection conditions". *Heat and Mass Transfer*, Vol. 42, pp. 1025–1036.

Harahap, F., Rudianto, E., & Pradnyana, I.M.E., 2005. "Measurements of steady-state heat dissipation from miniaturized horizontally-based straight rectangular fin arrays". *Heat and Mass Transfer*, Vol. 41(3), pp. 280-288.

Incropera, F.P., DeWitt, D.P., Bergman, T.L., & Lavine, A.S., 2008. *Fundamentos de Transferência de Calor e Massa*. 6ª edição. Rio de Janeiro: LTC.

Khor, Y.K., Hung, Y.M., & Lim, B.K., 2010. "On the role of radiation view factor in thermal performance of straight-fins. *International Communications in Heat and Mass Transfer*, Vol. 37(8), pp. 1087-1095.

Kobus, C.J., Oshio, T., 2005. "Predicting the thermal performance characteristics of staggered vertical pin fin array heat sinks under combined mode radiation and mixed convection with impinging flow". *International Journal of Heat and Mass Transfer*, Vol. 48, pp. 2684–2696.

Mehrtash, M., & Tari, I. (2013). "A correlation for natural convection heat transfer from inclined plate-finned heat sinks". *Applied Thermal Engineering*, Vol. 51(1-2), pp. 1067-1075.

Meng, X., Zhu, J., Wei, X., & Yan, Y., 2018. "Natural convection heat transfer of a straight-fin heat sink". *International Journal of Heat and Mass Transfer*, Vol. 123, pp. 561-568.

Rao, V.D., Naidu, S.V., Rao, B.G., & Sharma, K.V., 2006. "Heat transfer from a horizontal fin array by natural convection and radiation-a conjugate analysis". *International Journal of Heat and Mass Transfer*, Vol. 49(19-20), pp. 3379-3391.

Rao, V.D., Naidu, S.V., Rao, B.G., Sharma, K.V., 2007. "Combined convection and radiation heat transfer from a fin array with a vertical base and horizontal fins". *Proceedings of the World Congress on Engineering and Computer Science*, San Francisco, USA.

Sasikumar, M., Balaji, C., 2002. "A holistic optimization of convecting-radiating fin systems". *Journal of Heat Transfer*, Vol. 124, pp. 1110–1116.

Shabany, Y., 2008. "Radiation heat transfer from plate-fin heat sinks". *Proceedings of 24th Annual IEEE Semiconductor Thermal Measurement and Management Symposium (SEMI-THERM 24)*, IEEE Transactions, San Jose, CA.

Shen, Q., Sun, D., Xu, Y., Jin, T., & Zhao, X., 2014. "Orientation effects on natural convection heat dissipation of rectangular fin heat sinks mounted on LEDs". *International Journal of Heat and Mass Transfer*, Vol. 75, pp. 462-469.

Silva, V.A., 2015. *Análise experimental da influência dos parâmetros geométricos de dissipadores na convecção natural*", Mestrado em Engenharia Mecânica, Universidade Federal de Itajubá.

Yazicioğlu, B., & Yüncü, H., 2007. "Optimum fin spacing of rectangular fins on a vertical base in free convection heat transfer". *Heat and Mass Transfer*, Vol. 44(1), pp. 11-21.

Yazicioğlu, B., Yüncü, H., 2009. "A Correlation for optimum fin spacing of vertically-based rectangular fin arrays subjected to natural convection heat transfer". *Journal of Thermal Science and Technology*, Vol. 29, pp. 99–105.

Yu, S.H., Lee, K.S., & Yook, S.J., 2010. "Natural convection around a radial heat sink". *International Journal of Heat and Mass Transfer*, Vol. 53(13-14), pp. 2935-2938.

Yu, S.H., Lee, K.S., & Yook, S.J., 2011. "Optimum design of a radial heat sink under natural convection". *International Journal of Heat and Mass Transfer*, Vol. 54(11-12), pp. 2499-2505.

8. RESPONSIBILITY NOTICE

The authors are the only responsible for the printed material included in this paper.